

# One-loop matching of $\Delta S = 2$ four-quark operators with improved staggered fermions

Thomas Becher

*Fermi National Accelerator Laboratory, P. O. Box 500, Batavia, IL 60510, USA\**

Elvira Gámiz

*Department of Physics and Astronomy, University of Glasgow, Glasgow G12 8QQ, UK<sup>†</sup>*

Kirill Melnikov

*Department of Physics and Astronomy, University of Hawaii, Honolulu, HI 96822, USA<sup>‡</sup>*

We compute  $\mathcal{O}(\alpha_s)$  lattice-to-continuum perturbative matching coefficients for the  $\Delta S = 2$  flavor changing four-quark operators for the Asqtad improved staggered action. In conjunction with lattice simulations with three flavors of light, dynamical quarks, our results yield an unquenched determination of  $B_K$ , the parameter that determines the amount of indirect CP violation in the neutral kaon system. Its value is an important input for the unitarity triangle analysis of weak decays.

PACS numbers: 11.15.Ha, 12.38.Bx, 13.25.Es

## I. INTRODUCTION

Lattice calculations have started extracting phenomenologically relevant results with high precision and controlled uncertainties [1]. This requires simulations with dynamical quarks, lattice actions with small discretization errors and good control over perturbative corrections. Effective field theory methods are an important tool to achieve these goals. They enable a judicious design of lattice actions with small discretization errors. On the other hand, the complicated form of improved lattice actions puts a burden on perturbative calculations required to match the output of lattice simulations to continuum physics. For the matching to be meaningful, perturbative calculations have to be performed with *exactly the same* action and operators, with which the non-perturbative simulations are done.

The purpose of the present paper is to compute the matching coefficients of the four-fermion  $\Delta S = 2$  operators relevant for  $K - \bar{K}$  mixing for the Asqtad lattice action, an improved staggered fermion action used in many of the current simulations with dynamical quarks. The strength of  $K - \bar{K}$  mixing is determined by the matrix element  $\langle \bar{K} | (\bar{s}d)_{V-A} (\bar{s}d)_{V-A} | K \rangle \sim B_K(\mu)$ , where  $\mu$  is the renormalization scale. The determination of  $B_K(\mu)$  has

become an important goal of lattice simulations, since a precise value of this parameter translates into a stringent constraint on the unitarity triangle. The current constraint is dominated by theoretical uncertainties, the largest being the uncertainty in the value of  $B_K$  [2]. The experimental input comes from  $K \rightarrow \pi\pi$  decays and has percent level precision [3].

Results of lattice calculations for  $B_K(2 \text{ GeV})$  have been summarized in [4, 5]; a central value of  $B_K(2 \text{ GeV}) = 0.58(4)$  from quenched determinations was advocated in [4]. The uncertainty associated with this value does not include the systematic error induced by quenching, i.e. neglecting the effects of dynamical fermions. The errors from quenching are presumed to be of the order of 15%, but are very hard to estimate reliably [6]. In order to go beyond this accuracy, the calculation needs to be performed with dynamical fermions. The virtue of the improved action for which we perform our calculation is that it allows for precise calculations with light, dynamical quarks. The action is used by the MILC collaboration [7] and consists of the Asqtad discretization of staggered quarks [8, 9] coupled to a Symanzik improved gluon action [10].

The nonperturbative calculation of the matrix elements of the lattice operators on the MILC dynamical configurations was discussed in [11], along with preliminary results for the bare  $B_K$  parameter. Together with the matching coefficients given in this paper, these results determine the renormalized continuum value  $B_K(\mu)$  [12].

In [13] two of us suggested an approach to lattice perturbation theory that allows an efficient separation of

\*Electronic address: becher@fnal.gov

<sup>†</sup>Electronic address: e.gamiz@physics.gla.ac.uk

<sup>‡</sup>Electronic address: kirill@phys.hawaii.edu

energy scales that appear in matching calculations – the inverse lattice spacing, which plays the role of the ultraviolet cut-off, and the physical masses and momenta. As a result of this scale separation, we are able to treat the complicated integrals that appear in lattice perturbation theory by algebraic means. The approach allows a very high degree of automation, thereby circumventing the complexity of improved lattice actions to a certain degree. We have used this method in [14] to compute the one-loop relation between the bare lattice mass and the pole mass for the Asqtad action. In the present paper we compute the matching coefficient for  $\Delta S = 2$  four-fermion operators for the Asqtad action, using the algebraic technique [13] as well as numerically. The agreement of the results obtained using these two completely different techniques provides a strong check on the calculation.

The lattice-to-continuum matching coefficients for the  $\Delta S = 2$  four-quark operators have been previously calculated for the standard, unimproved, discretization of staggered fermions [15], as well as for a class of improved staggered actions [16]. While none of these results is directly relevant for the Asqtad action, we have checked that we reproduce the known result for the unimproved action, once we switch off all improvement terms.

The rest of the paper is organized as follows. In the next Section we give the discretization of the four-fermion operators. In Section III we discuss how the matching is performed and give the result for each of the relevant Feynman diagrams. In Section IV we include the tadpole improvement terms. We present our results for the matching coefficients that relate bare lattice operators to continuum  $\overline{MS}$  operators in Section V. Finally, in the last Section we summarize our results and compare the size of the perturbative corrections found for different staggered actions.

## II. STAGGERED AND NAIVE LATTICE OPERATORS

For energy scales below the charm quark mass, the continuum effective Hamiltonian relevant for  $K - \bar{K}$  mixing reads [17]

$$H_{\text{eff}}^{\text{weak}} = \frac{G_F^2 m_W^2}{16\pi^2} C(\mu) Q(\mu), \quad (1)$$

where

$$Q = (\bar{s}d)_{V-A} (\bar{s}d)_{V-A}. \quad (2)$$

The possibility to describe  $K - \bar{K}$  mixing by a single operator is a consequence of the  $V - A$  structure of weak interactions and the Fierz identities that facilitate expressing any relevant four-quark operator in canonical form (2).

Lattice simulations of the  $K - \bar{K}$  mixing require introducing the operator  $Q$  on the lattice. It is convenient to perform the perturbative calculations with naive

instead of staggered quarks and to carry out the spin-diagonalization and the reduction from the sixteen to four doublers (or “tastes”) afterwards. We use the standard discretization for the staggered four-quark operators and now show how these operators can be rewritten in terms of the naive fermion field.

The naive fermion field  $\psi$  and the staggered field  $\chi$  at lattice site  $n = (n_1, n_2, n_3, n_4)$  are related by

$$\psi(n) = \Gamma_n \chi(n) \quad \bar{\psi}(n) = \bar{\chi}(n) \Gamma_n^\dagger \quad (3)$$

where

$$\Gamma_n = (\gamma_1)^{n_1} (\gamma_2)^{n_2} (\gamma_3)^{n_3} (\gamma_4)^{n_4}. \quad (4)$$

We choose a Hermitian representation of the Euclidean Dirac algebra with

$$\{\gamma_i, \gamma_j\} = 2\delta_{ij} \quad \text{and} \quad \gamma_5 = \gamma_1 \gamma_2 \gamma_3 \gamma_4. \quad (5)$$

When written in terms of staggered fermions, the quark action becomes spin diagonal and three of the four components of the quark field  $\chi$  can be dropped. In perturbation theory it is more convenient to keep all components, and replace  $n_f \rightarrow n_f/4$  at the end of the calculations to obtain the result for the single component field.

The fields  $\chi(2N + A)$  are collected into a set of Dirac fields  $q(2N)$  that live on the even lattice sites and are spread over a unit hypercube [18, 19, 20] ( $A_\mu = 0$  or  $1, \mu = 1 \dots 4$ )

$$q(2N)_{\alpha ij} = \frac{1}{8} \sum_A (\Gamma_A)_{\alpha, i} \chi_j(2N + A). \quad (6)$$

The index  $\alpha$  is the Dirac index of the new field and  $i$  the “taste” index. The second taste index  $j$  runs over the components of the field  $\chi$ . Staggered fermions have only one component, while the four component of the naive field give rise to  $4 \times 4$  tastes. Bilinear quark operators with spin structure  $\gamma_S$  and taste structure  $\xi_T = \Gamma_T^*$  (with  $T$  again on the unit hypercube) are

$$\begin{aligned} & \bar{q}(2N)(\gamma_S \otimes \xi_T)q(2N) \\ &= \frac{1}{16} \sum_{A,B} \bar{\chi}(2N + A) \chi(2N + B) \frac{1}{4} \text{tr}(\Gamma_A^\dagger \gamma_S \Gamma_B \Gamma_T^\dagger). \end{aligned} \quad (7)$$

Since the quark fields in the operators are at different lattice points, they need to be connected by Wilson lines in order to make the operators gauge invariant. We suppress these Wilson lines, but it is understood that gauge strings among all possible shortest paths connecting the quark fields are inserted and the operator is divided by the number of paths. Using (3) we rewrite the operator in terms of the naive fermion field:

$$\begin{aligned} & \bar{q}(2N)(\gamma_S \otimes \xi_T)q(2N) \\ &= \frac{1}{16} \sum_{A,B} \bar{\psi}(2N + A) \Gamma_A \Gamma_B^\dagger \psi(2N + B) \frac{1}{4} \text{tr}(\Gamma_A^\dagger \gamma_S \Gamma_B \gamma_T^\dagger). \end{aligned} \quad (8)$$

Let us write out the vector and axial currents at  $N = 0$  with unit taste structure in terms of the naive quark field  $\psi(n)$ . We find

$$\bar{q}(\gamma_\mu \otimes 1)q = \frac{1}{16} \sum_A \delta_{A\mu,0} [\bar{\psi}(A)\gamma_\mu\psi(A + \hat{\mu}) + \bar{\psi}(A + \hat{\mu})\gamma_\mu\psi(A)], \quad (9)$$

and  $(\bar{A} = (1, 1, 1, 1) - A)$

$$\bar{q}(\gamma_\mu\gamma_5 \otimes 1)q = \frac{1}{16} \sum_A \delta_{A\mu,0} [\bar{\psi}(A)\gamma_\mu\gamma_5\psi(\bar{A} + \hat{\mu}) + \bar{\psi}(\bar{A})\gamma_\mu\gamma_5\psi(A + \hat{\mu})]. \quad (10)$$

In the continuum limit, the massless staggered action has a  $SU(4)_L \times SU(4)_R$  chiral symmetry (for a single staggered field) and one would naively expect to find fifteen Goldstone bosons after chiral symmetry breaking, corresponding to the fifteen traceless taste matrices. However, this symmetry is explicitly broken to an axial  $U(1)$  symmetry by terms in the action proportional to the lattice spacing squared. The generator of the remaining axial symmetry is the matrix  $\gamma_S \otimes \xi_T = \gamma_5 \otimes \gamma_5$ . In our case, this implies that only the kaon with taste structure  $\gamma_5$  becomes massless in the chiral limit. For this reason, the simulation is done with currents having  $\xi_T = \gamma_5$  taste structure and not the unit matrix as in (9) and (10). However, it has been shown that the result for diagrams in which the fermions in the operators are not contracted are identical for the Dirac and taste structures  $\Gamma \otimes \Gamma'$  and  $\Gamma\gamma_5 \otimes \Gamma'\gamma_5$  [20].<sup>1</sup> For our perturbative calculation we will thus use (10) instead of the vector current  $\gamma_\mu \otimes \gamma_5$  and (9) in place of  $\gamma_\mu\gamma_5 \otimes \gamma_5$ .

The operator  $Q$  for which we want to perform the matching calculation is a product of two  $V - A$  currents. We will see that QCD corrections to bare lattice four-quark operators affect the vector and axial parts differently; as a consequence currents of the form  $V + A$  are generated. A minimal set of lattice operators that matches to the continuum and closes under renormalization consists of 4 scalar and 2 pseudoscalar operators. Schematically these operators are

$$\begin{aligned} Q_1 &= (\bar{s}^a d^a)_V (\bar{s}^b d^b)_V, & Q_2 &= (\bar{s}^a d^b)_V (\bar{s}^b d^a)_V, \\ Q_3 &= (\bar{s}^a d^a)_A (\bar{s}^b d^b)_A, & Q_4 &= (\bar{s}^a d^b)_A (\bar{s}^b d^a)_A, \\ Q_5 &= (\bar{s}^a d^a)_V (\bar{s}^b d^b)_A + (\bar{s}^a d^a)_A (\bar{s}^b d^b)_V, \\ Q_6 &= (\bar{s}^a d^b)_V (\bar{s}^b d^a)_A + (\bar{s}^a d^b)_A (\bar{s}^b d^a)_V. \end{aligned} \quad (11)$$

$V$  and  $A$  are the vector and axial currents with taste structure  $\xi_T = \gamma_5$ . The color indices  $a, b$  indicate which

fields are connected by Wilson lines. The pseudoscalar operators  $Q_{5,6}$  only mix amongst themselves and their  $K - \bar{K}$  matrix element vanishes, because of parity. In the following we will therefore only consider the renormalization of the operators  $Q_{1-4}$ .

The above operators are used in the nonperturbative calculation of the matrix elements by the HPQCD collaboration [11, 12]. In contrast to the lattice action, these operators are not Symanzik improved.

### III. MATCHING CALCULATION

To perform the matching we calculate a physical quantity in the continuum and on the lattice, expand around the continuum limit, and adjust the Wilson coefficients of the lattice operators in such a way that they reproduce the continuum result. Specifically, we determine the bare lattice Wilson coefficients from the quark-quark scattering amplitude

$$\mathcal{A} = Z^2 C_i^{\text{bare}} \langle O_i^{\text{bare}} \rangle = Z^2 C_i Z_{ij} \langle O_j \rangle = Z_{\text{lat}}^2 C_i^{\text{lat}} \langle O_i^{\text{lat}} \rangle, \quad (12)$$

where  $Z$  and  $Z_{\text{lat}}$  are on-shell quark wave-function renormalizations and  $\langle O \rangle$  is the amputated four-quark Green's function with an insertion of the operator  $O$ . The lattice-to-continuum matching coefficients are independent of the quantity chosen to perform the matching. At one-loop order, it is simplest to regulate infrared divergencies with a gluon mass and to calculate the scattering amplitude of massless quarks at zero external momentum.

At tree level in the continuum limit, the operators  $Q_i$  are identical to their continuum counterparts; this implies that no tree level matching is required. At one loop the matching coefficients  $C_i^{\text{lat}}$  are obtained by calculating the difference between the lattice and continuum one-loop diagrams. In the difference, the infrared divergencies cancel. Below we present such a calculation for the set of lattice operators described above.

For unimproved staggered fermions the renormalization of the axial current operator with  $\gamma_S \otimes \xi_T = \gamma_\mu \gamma_5 \otimes \gamma_5$  is finite and identical in the continuum and on the lattice. This happens because it renormalizes in the same way as the vector current with unit taste structure  $\gamma_\mu \otimes 1$  which has exactly the same form as the quark-gluon coupling in the Lagrangian. Because of the improvement terms, this is not true for the Asqtad action and we will need to evaluate the matching not only for the four-quark operators but also for the current.

The matching calculation requires computing matrix elements of certain operators in lattice perturbation theory; to do so we use the approach described in [13, 14]. In those references an expansion of the lattice integrals around the continuum limit is introduced by utilizing the technique of asymptotic expansions. The asymptotic expansion around the continuum limit splits the lattice diagrams into two parts: (i) a soft part which is obtained by

<sup>1</sup> The reason is that in this case, one can view the four fermions as four different quark flavors and perform separate axial  $U(1)$  transformations on each field.

evaluating continuum loop integrals (in analytic regularization) and is independent of the discretization and (ii) a hard part which depends on the discretization but is independent of particle masses and momenta. The proximity of the soft part of the lattice loop integrals and the continuum integrals in dimensional regularization permits significant simplifications when computing the difference of the lattice and continuum Green's functions required for matching calculations.

There are five diagrams (plus permutations) that contribute at  $\mathcal{O}(\alpha_s)$  to the quark-quark scattering amplitude; they are shown in Fig. 1. To present the result of the calculations, we introduce the following notation for the difference of the lattice and continuum one-loop matrix elements of the four-fermion operators:

$$\delta\langle Q^i \rangle_\alpha = \left(\frac{\alpha_s}{4\pi}\right) \left(\frac{\mu a}{2}\right)^{2\epsilon} \sum_{j=1}^4 q_{\alpha,j}^i Q^j, \quad (13)$$

where the label  $\alpha$  refers to a particular diagram shown in Fig. 1. The spacetime dimension is  $d = 4 - 2\epsilon$ ,  $\mu$  is the renormalization scale in the  $\overline{\text{MS}}$  subtraction scheme and  $a$  the lattice spacing. In what follows, we split the matrices  $q_i$  into soft and hard pieces. We give the result for each diagram separately. We hope that the results for the individual diagrams will be useful for readers performing similar calculations in the future.

### A. Soft part

As a first step in the matching calculation, we compute the difference between the soft parts of lattice matrix elements and the result derived in dimensional regularization. To obtain the full result, we later add the hard part for a given lattice action. Technically the soft part is obtained by evaluating the continuum diagrams shown in Fig. 1, first in dimensional and then in analytic regularization. The calculation is simplified by noting that a difference between the two regulators can only arise from ultraviolet divergent loop integrals.

Below we give the results for the *difference* of the soft parts of the matrices  $q$  and the corresponding continuum diagrams. Since the diagrams 4 and 5 in Fig. 1 do not have continuum analog, their contribution to the soft part is zero:  $q_4^{\text{soft}} = q_5^{\text{soft}} = 0$ . For diagram 1, we derive

$$q_1^{\text{soft}} = \begin{pmatrix} C_F f_{11}^{(1)} & 0 & 0 & 0 \\ \frac{f_{11}^{(1)}}{2} & -\frac{f_{11}^{(1)}}{2N} & 0 & 0 \\ 0 & 0 & C_F f_{11}^{(1)} & 0 \\ 0 & 0 & \frac{f_{11}^{(1)}}{2} & -\frac{f_{11}^{(1)}}{2N} \end{pmatrix}.$$

The variable  $N = 3$  denotes the number of colors,  $C_F = (N^2 - 1)/2N$  and

$$f_{11}^{(1)} = -2(1 + \xi) \left(\frac{1}{\epsilon} - \frac{1}{\delta}\right) + 1 - 2\xi. \quad (14)$$

The parameter  $\delta$  is an intermediate analytic regulator, which will drop out in the sum of the hard and soft part [13]. Setting the gauge parameter  $\xi = 0$ , one obtains the result in Feynman gauge while  $\xi = -1$  corresponds to Landau gauge. For details on our notation and method of calculation, we refer the reader to [14].

For diagrams 2 and 3 in Fig. 1 we obtain,

$$q_2^{\text{soft}} = \begin{pmatrix} -\frac{f_{11}^{(2)}}{2N} & \frac{f_{11}^{(2)}}{2} & -\frac{f_{13}^{(2)}}{2N} & \frac{f_{13}^{(2)}}{2} \\ \frac{f_{11}^{(2)}}{2} & -\frac{f_{11}^{(2)}}{2N} & \frac{f_{13}^{(2)}}{2} & -\frac{f_{13}^{(2)}}{2N} \\ -\frac{f_{13}^{(2)}}{2N} & \frac{f_{13}^{(2)}}{2} & -\frac{f_{11}^{(2)}}{2N} & \frac{f_{11}^{(2)}}{2} \\ \frac{f_{13}^{(2)}}{2} & -\frac{f_{13}^{(2)}}{2N} & \frac{f_{11}^{(2)}}{2} & -\frac{f_{11}^{(2)}}{2N} \end{pmatrix},$$

$$q_3^{\text{soft}} = \begin{pmatrix} -\frac{f_{11}^{(3)}}{2N} & \frac{f_{11}^{(3)}}{2} & -\frac{f_{13}^{(3)}}{2N} & \frac{f_{13}^{(3)}}{2} \\ 0 & C_F f_{11}^{(3)} & 0 & C_F f_{13}^{(3)} \\ -\frac{f_{13}^{(3)}}{2N} & \frac{f_{13}^{(3)}}{2} & -\frac{f_{11}^{(3)}}{2N} & \frac{f_{11}^{(3)}}{2} \\ 0 & C_F f_{13}^{(3)} & 0 & C_F f_{11}^{(3)} \end{pmatrix},$$

where

$$\begin{aligned} f_{11}^{(2)} &= -f_{11}^{(3)} + 6 = (5 + 2\xi) \left(\frac{1}{\epsilon} - \frac{1}{\delta}\right) + \frac{15}{2} + 2\xi, \\ f_{13}^{(2)} &= f_{13}^{(3)} = 3 \left(\frac{1}{\epsilon} - \frac{1}{\delta}\right) + \frac{5}{2}. \end{aligned} \quad (15)$$

To evaluate the continuum diagrams, a prescription for the treatment of  $\gamma_5$  and the extension of the Fierz identities to  $d$ -dimensions [21, 22, 23] has to be adopted. We use naive dimensional regularization for  $\gamma_5$  and treat the evanescent operators exactly as in [17], to be compatible with the results for the Wilson coefficients given in these references. Note that with this prescription, the operators  $Q_1 \propto \gamma_\mu \otimes \gamma_\mu$  and  $Q_3 \propto \gamma_\mu \gamma_5 \otimes \gamma_\mu \gamma_5$  also mix into operators with Dirac structure  $1 \otimes 1$ ,  $\gamma_5 \otimes \gamma_5$  and  $\sigma_{\mu\nu} \otimes \sigma_{\mu\nu}$ . We do not give the result for this mixing, since it drops out in the sums  $Q_1 + Q_3$  and  $Q_2 + Q_4$  which are relevant for our matching calculation. However, separating the vector and axial contributions also in the soft part allows us to read off the current renormalizations from the first diagram in Fig. 1 and provides additional consistency checks, such as cancellation of  $\delta$ -poles and gauge invariance of the sum of hard and soft parts.

In addition to the diagrams shown in Fig. 1, we have to account for the external leg corrections, given by the wave function renormalization of the massless quarks. This correction is universal in that it does not depend on the operator under consideration. We obtain

$$\delta Z^{(1)} O_i|_{\text{soft}} = C_F \left(\frac{2}{\epsilon} - \frac{2}{\delta} + 1\right) (1 + \xi) O_i, \quad (16)$$

where  $Z_{\text{lat}}^2 - Z^2 = \frac{\alpha_s}{\pi} \delta Z^{(1)} + \dots$  is the difference between the lattice (soft part only) and the on-shell quark wave function renormalization constant. This difference vanishes in Landau gauge, which is a consequence of the fact

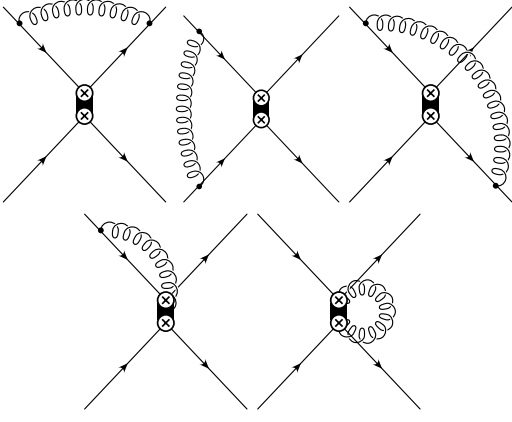


FIG. 1: Current-current diagrams. The diagrams on the second line do not have a continuum analog. Not shown are additional diagrams that can be obtained by flipping one of the above diagrams horizontally or vertically.

that in this gauge the continuum quark wave function renormalization is finite.

Note that the coefficients of the  $1/\epsilon$  and  $1/\delta$  pieces in all the equations above are exactly opposite. The  $1/\delta$ -divergences will cancel against those of the hard parts. The fact that the above differences do not depend on any infrared scales (the gluon mass in our case) shows that the result of a matching calculation is process independent.

### B. Hard part

We now give the result of our calculation of the hard part. This amounts to presenting the matrices  $q_\alpha$  for the five diagrams in Fig. 1. The symmetry factors for each of the diagrams are included. We begin with naive unimproved fermions coupled to unimproved glue.

The result for the hard part of the first three diagrams in Fig. 1, has the same structure as was found for the soft part:

$$q_1^{\text{hard}} = \begin{pmatrix} C_F d_{11}^{(1)} & 0 & 0 & 0 \\ \frac{d_{11}^{(1)}}{2} & -\frac{d_{11}^{(1)}}{2N} & 0 & 0 \\ 0 & 0 & C_F d_{33}^{(1)} & 0 \\ 0 & 0 & \frac{d_{33}^{(1)}}{2} & -\frac{d_{33}^{(1)}}{2N} \end{pmatrix},$$

where

$$\begin{aligned} d_{11}^{(1)} &= -\frac{2(1+\xi)}{\delta} - 3.53 - 2.38\xi, \\ d_{33}^{(1)} &= -\frac{2(1+\xi)}{\delta} - 3.62 + 0.695\xi, \end{aligned} \quad (17)$$

and

$$q_2^{\text{hard}} = \begin{pmatrix} -\frac{d_{11}^{(2)}}{2N} & \frac{d_{11}^{(2)}}{2} & -\frac{d_{13}^{(2)}}{2N} & \frac{d_{13}^{(2)}}{2} \\ \frac{d_{11}^{(2)}}{2} & -\frac{d_{11}^{(2)}}{2N} & \frac{d_{13}^{(2)}}{2} & -\frac{d_{13}^{(2)}}{2N} \\ -\frac{d_{13}^{(2)}}{2N} & \frac{d_{13}^{(2)}}{2} & -\frac{d_{11}^{(2)}}{2N} & \frac{d_{11}^{(2)}}{2} \\ \frac{d_{13}^{(2)}}{2} & -\frac{d_{13}^{(2)}}{2N} & \frac{d_{11}^{(2)}}{2} & -\frac{d_{11}^{(2)}}{2N} \end{pmatrix},$$

$$q_3^{\text{hard}} = \begin{pmatrix} -\frac{d_{11}^{(3)}}{2N} & \frac{d_{11}^{(3)}}{2} & -\frac{d_{13}^{(3)}}{2N} & \frac{d_{13}^{(3)}}{2} \\ 0 & C_F d_{11}^{(3)} & 0 & C_F d_{13}^{(3)} \\ -\frac{d_{13}^{(3)}}{2N} & \frac{d_{13}^{(3)}}{2} & -\frac{d_{11}^{(3)}}{2N} & \frac{d_{11}^{(3)}}{2} \\ 0 & C_F d_{13}^{(3)} & 0 & C_F d_{11}^{(3)} \end{pmatrix},$$

with

$$\begin{aligned} d_{11}^{(2)} &= -d_{11}^{(3)} = \frac{(5+2\xi)}{\delta} + 0.157 + 0.689\xi, \\ d_{13}^{(2)} &= d_{13}^{(3)} = \frac{3}{\delta} - 0.341, \end{aligned} \quad (18)$$

The remaining two diagrams have no continuum analogue. We obtain

$$q_{i=4,5}^{\text{hard}} = \begin{pmatrix} C_F d_{11}^{(i)} & 0 & 0 & 0 \\ d_{21}^{(i)} & C_F d_{22}^{(i)} - \frac{d_{21}^{(i)}}{N} & 0 & 0 \\ 0 & 0 & C_F d_{33}^{(i)} & 0 \\ 0 & 0 & d_{43}^{(i)} & C_F d_{44}^{(i)} - \frac{d_{43}^{(i)}}{N} \end{pmatrix},$$

with entries

$$\begin{aligned} d_{11}^{(4)} &= 16.06 + 18.38\xi, \\ d_{21}^{(4)} &= 1.18 + 1.69\xi, \\ d_{22}^{(4)} &= 13.70 + 15.00\xi, \\ d_{33}^{(4)} &= 12.23 + 12.23\xi, \\ d_{43}^{(4)} &= -0.73 - 1.38\xi, \\ d_{44}^{(4)} &= 13.70 + 15.00\xi, \end{aligned} \quad (19)$$

$$\begin{aligned} d_{11}^{(5)} &= -73.40 - 9.19\xi, \\ d_{21}^{(5)} &= -2.20 - 0.85\xi, \\ d_{22}^{(5)} &= -48.9 - 7.50\xi, \\ d_{33}^{(5)} &= -24.47 - 6.12\xi, \\ d_{43}^{(5)} &= 1.57 + 0.69\xi, \\ d_{44}^{(5)} &= -48.9 - 7.50\xi. \end{aligned} \quad (20)$$

We also give the result for the hard part fermion wave function renormalization on the lattice:

$$\begin{aligned} \delta Z^{(1)} O_i|_{\text{hard}} &= C_F \left( -10.614 - 11.928\xi + \frac{2(1+\xi)}{\delta} \right. \\ &\quad \left. + [24.466 + 6.117\xi] \right) O_i. \end{aligned} \quad (21)$$

We have separated out the tadpole contribution in (21) in square brackets. In Landau gauge this contribution exactly cancels against the tadpole improvement term.

We now give the results for the entries of the matrices for the case of Asqtad action. In this case, as explained in [14], we expand in the improvement terms, for both quark and gluon actions. We use half of the highest order terms as the numerical error estimate and multiply the last term of the series by 2/3 to resum the higher order contributions that behave like an alternating geometric series with expansion parameter 1/2 (see [14] for details). We find

$$\begin{aligned}
d_{11}^{(1)} &= -\frac{2(1+\xi)}{\delta} - 3.00(1) - 2.379\xi, \\
d_{33}^{(1)} &= -\frac{2(1+\xi)}{\delta} + 0.81(4) + 0.695\xi \\
d_{11}^{(2)} &= -d_{11}^{(3)} = \frac{(5+2\xi)}{\delta} + 2.79(10) + 0.689\xi, \\
d_{13}^{(2)} &= d_{13}^{(3)} = \frac{3}{\delta} + 2.10(9), \\
\\
d_{11}^{(4)} &= 18.54(6) + 18.38\xi, \\
d_{21}^{(4)} &= 1.73(1) + 1.69\xi, \\
d_{22}^{(4)} &= 15.09(3) + 15.00\xi, \\
d_{33}^{(4)} &= 12.23 + 12.23\xi, \\
d_{43}^{(4)} &= -1.43(2) - 1.38\xi, \\
d_{44}^{(4)} &= 15.09(3) + 15.00\xi, \\
\\
d_{11}^{(5)} &= -58.0(5) - 9.19\xi, \\
d_{21}^{(5)} &= -2.06 - 0.84\xi, \\
d_{21}^{(5)} &= -39.1(3) - 7.50\xi, \\
d_{33}^{(5)} &= -20.3(1) - 6.12\xi, \\
d_{43}^{(5)} &= 1.56(1) + 0.69\xi, \\
d_{44}^{(5)} &= -39.1(3) - 7.50\xi.
\end{aligned} \tag{22}$$

The gauge dependent part is the same as in the unimproved case because the improvement terms in the action are transverse [14].

For the Asqtad action, the wave function renormalization contribution is:

$$\begin{aligned}
\delta Z^{(1)} O_i|_{\text{hard}} &= C_F \left( -14.3(2) - 11.28\xi + \frac{2(1+\xi)}{\delta} \right. \\
&\quad \left. + [30.1(6) + 5.47\xi] \right) O_i.
\end{aligned} \tag{23}$$

The renormalization of the axial and vector current can be read off from the above expressions. In both cases it is given by one half of the corresponding entries in the matrices  $q_i$  for diagrams 1, 4 and 5 in Fig. 1 and the contribution due to the wave function renormalization. As

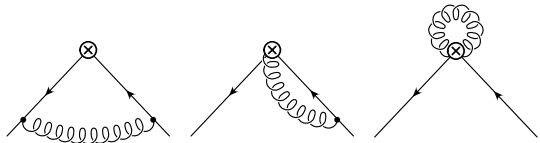


FIG. 2: Current diagrams.

discussed earlier in this section, the discretized version of the axial current that we use in this paper renormalizes identically to the unimproved quark-gluon vertex. As a consequence, the lattice-to-continuum matching coefficient for the axial current should be equal to unity for the unimproved action, to all orders in  $\alpha_s$ . Using the results presented above, it is easy to verify this at the one-loop level.

### C. Matching coefficients from a different method

Most of the diagrams needed in the determination of the matching coefficients for four-fermion operators can be calculated from the renormalization coefficients for bilinears operators, as was first pointed out by Martinelli [24]. The method has been generalized to Landau-gauge operators in [20], general local operators in [25] and staggered gauge invariant operators in [16].

In Fig. 1, we did not show mirrored diagrams and did not display the color structure of the four-quark operators. Also, we have not indicated from which of the two currents the gluons in diagrams 4 and 5 are emitted. Listing all possibilities, one ends up with 16 diagrams of type 4 and 6 of type 5. Only 8 of the 16 diagrams of type 4 and 2 of the 6 diagrams of type 5 are genuine four-fermion contributions. All other diagrams factor into a product of a one-loop current renormalization diagram times a tree level current. Furthermore, only half of the remaining diagrams contribute to the mixing between operators whose bilinears have identical taste-structure, which is all that is relevant for matrix elements involving external states of definite taste. One cannot avoid calculating the genuine four-fermion diagrams, but the result for the other topologies can be obtained from the diagonal renormalization coefficients for bilinears operators using Fierz and charge conjugation transformations as described in [16]. Apart from the 5 genuine four-fermion diagrams, the calculation reduces to the evaluation of the current renormalization diagrams in Fig. 2 and the universal wave function renormalization of the massless quarks. In Fig. 2, the crossed circle denotes the insertion of any bilinear with structure  $(\gamma_S \otimes \xi_T)$ . The calculation is further simplified by noting that the corrections are identical if the operators are multiplied by  $(\gamma_5 \otimes \gamma_5)$  due to the axial symmetry, as stressed above.

For diagonal four-fermion operators (with identical taste and spin structure in both bilinears) this procedure gives us a  $35 \times 35$  matrix from which we can extract the

$2 \times 2$  block describing the mixing between  $[\gamma_\mu \otimes \gamma_5][\gamma_\mu \otimes \gamma_5]$  and  $[\gamma_\mu \gamma_5 \otimes \gamma_5][\gamma_\mu \gamma_5 \otimes \gamma_5]$ . This block is related to the  $4 \times 4$  matrix in (32) by including the appropriate color factors as explained in [16].

We have done the calculation of the matching coefficients for the  $\Delta S = 2$  four-quark operators using the method described above and evaluating the integrals numerically instead of algebraically. In all cases we find full agreement with the direct evaluation of the diagrams. This independent calculation of the matching coefficients provides a non-trivial check of the validity of our results. In addition, we have also performed the calculation for the HYP actions used in [16] and reproduce the result for the matching matrix given in that reference.

#### IV. TADPOLE IMPROVEMENT

Quite generally one finds that perturbative corrections in lattice regularization are larger than those encountered in continuum calculations, e.g. in the  $\overline{\text{MS}}$  scheme. The large corrections typically arise from the additional diagrams that would be absent in the continuum, in our case the fourth and fifth diagram in Fig. 1. Since the size of the corrections is scheme dependent they are not by themselves meaningful. Instead of just working with the bare lattice parameters one can try to absorb the large perturbative corrections into a redefinition of the basic parameters of the theory, such as coupling constant, quark masses, Wilson coefficients of the weak Hamiltonian, etc. Such techniques are also used in the continuum, for example in the context of Heavy-Quark Effective theories: the perturbative results for inclusive heavy hadron decay rates get large perturbative corrections if they are expressed in terms of the heavy quark pole mass but the corrections are much smaller if one uses a more suitable mass definition [26, 27, 28]. Similar ideas are behind the so-called ‘‘physical’’ couplings and optimal scale setting prescriptions, introduced quite some time ago [29].

The large effects of the tadpole diagrams can be canceled by tadpole improvement [30]. Tadpole improvement is achieved by working with an action in which all gauge links are divided by an average link  $u_0$ . In the simulation the average link is determined numerically, while it is evaluated perturbatively in the matching calculation. We define

$$u_0 = 1 - \alpha_s u_0^{(1)} + \dots \quad (24)$$

The average link receives large perturbative corrections which then cancel out the large contributions from the tadpole diagrams. In this section we give the tadpole improvement terms relevant for our calculation. Some care is required because different variants of tadpole improvement are used in the literature. First of all, two different definitions of the the mean link  $u_0$  are common:

the mean link in Landau gauge

$$u_0 = \left\langle \frac{1}{3} \text{Re Tr } U_{n,\mu} \right\rangle_{\xi=-1} \quad (25)$$

or the fourth root of the average plaquette

$$u_0^P = \left\langle \frac{1}{3} \text{Re Tr } U_{n,\mu} U_{n+\mu,\nu} U_{n+\mu+\nu,\mu}^\dagger U_{n+\nu,\nu}^\dagger \right\rangle^{1/4}. \quad (26)$$

The second definition is somewhat simpler since no gauge fixing is required and it is what MILC is using in their simulations with the Asqtad action. Furthermore, MILC divides the  $L$ -link terms in the action and operators not by  $u_0^L$  as [30] but by  $u_0^{L-1}$  and absorbs a power of  $u_0$  into the fermion mass. With their prescription no tadpole improvement factor is present in the fermion part of the naive unimproved action [9].<sup>2</sup> Since the fermion mass does not enter our calculation, the difference between the two prescriptions merely amount to a rescaling of the fermion field and leads to identical results for the matching coefficients we calculate.

If we divide the  $L$ -link terms by  $u_0^L$ , the tadpole improvement contribution from the current operators is

$$q^{(\text{tad})} = 4\pi u_0^{(1)} \begin{pmatrix} 6 & 0 & 0 & 0 \\ 0 & 4 & 0 & 0 \\ 0 & 0 & 2 & 0 \\ 0 & 0 & 0 & 4 \end{pmatrix}. \quad (27)$$

In addition, there is a tadpole improvement correction to the square of the wave function renormalization

$$\begin{aligned} \delta Z_{\text{unimp}}^{\text{tad}} Q_i &= -8\pi u_0^{(1)} Q_i, \\ \delta Z_{\text{Asqtad}}^{\text{tad}} Q_i &= -18\pi u_0^{(1)} Q_i. \end{aligned} \quad (28)$$

The results given in the next section are obtained with  $u_0$  defined as the mean link in Landau gauge (25). However, using the explicit form of the tadpole improvement terms given above the prescription can easily be changed.

#### V. WILSON COEFFICIENTS OF THE LATTICE OPERATORS

The Wilson coefficients of the lattice operators can now be read off by imposing that the four-quark scattering amplitudes are equal in the continuum and on the lattice. Clearly, the solution to the matching equation (12) is in general not unique since there are many different discretizations of the same continuum operator. In the present case, the two  $(\bar{s}d)_{V-A}(\bar{s}d)_{V-A}$  operators with different color structure become equivalent in the continuum limit where they are related by a Fierz transformation. The matching condition will thus not fix the Wilson

<sup>2</sup> We thank C. Bernard for pointing this out to us.

coefficients of the operators with different color structure individually. To be specific, at tree level the matching conditions impose only three relations

$$\begin{aligned} C_1^{\text{latt}} &= C_3^{\text{latt}} + \mathcal{O}(\alpha_s), \\ C_2^{\text{latt}} &= C_4^{\text{latt}} + \mathcal{O}(\alpha_s), \\ C^{\text{cont}} &= C_1^{\text{latt}} + C_2^{\text{latt}} + \mathcal{O}(\alpha_s), \end{aligned} \quad (29)$$

among the four lattice operator Wilson coefficients. Here,  $C^{\text{cont}}$  is the Wilson coefficient of the continuum operator  $Q$ , while  $C_i^{\text{latt}}$  are the coefficients of  $Q_i$ .

In lattice simulations, the quarks in the operator  $Q$  are treated as four distinct flavors [31]. In this case, there is no ambiguity: the effective continuum Hamiltonian contains operators  $Q_i^{\text{cont}}$  that are the continuum limit of each  $Q_i$ . Also, instead of writing relations among coefficients, it is more convenient to rewrite the result of the matching in the form

$$Q_i^{\text{cont}} \equiv \sum_{j=1}^4 C_{ij} Q_j^{\text{lat}}, \quad (30)$$

where “ $\equiv$ ” means equality at the level of matrix elements, see (12). The 4 by 4 matrix  $C_{ij}$  has a perturbative expansion

$$C_{ij} = \delta_{ij} + \left(\frac{\alpha_s}{\pi}\right) C_{ij}^{(1)} + \dots \quad (31)$$

and is obtained from the results for the graphs in the previous section by

$$C_{ij}^{(1)} = -\frac{1}{4} \left[ \delta Z^{(1)} \delta_{ij} + \left(\frac{a\mu}{2}\right)^{2\epsilon} \sum_{\alpha} q_{\alpha,j}^i + \delta Z_{ij}^{(1)} \right]. \quad (32)$$

Here  $\delta Z^{(1)}$  stands for the wave function renormalization and  $Z_{ij} = \delta_{ij} + \frac{\alpha_s}{\pi} Z_{ij}^{(1)}$  is the matrix of the  $\overline{\text{MS}}$  renormalization constants for the operators  $Q_i^{\text{cont}}$  in the continuum. For the purposes of computing  $C_{ij}^{(1)}$ , the role of this matrix is to remove any residual  $1/\epsilon$  dependence in (32). Using the results for the matrices  $q_{\alpha}$  given in the previous section, it is straightforward to compute the matching coefficients. We split the matrix  $C_{ij}^{(1)}$  into three parts

$$C^{(1)} = \ln\left(\frac{a\mu}{2}\right) \gamma^{(1)} + C_C^{(1)} + C_U^{(1)}. \quad (33)$$

Here,  $\gamma^{(1)}$  is the universal one-loop anomalous dimensions matrix of the operators  $Q_i$ :

$$\gamma^{(1)} = \begin{pmatrix} 0 & 0 & \frac{1}{2} & -\frac{3}{2} \\ -\frac{3}{4} & \frac{9}{4} & -\frac{3}{4} & -\frac{7}{4} \\ \frac{1}{2} & -\frac{3}{2} & 0 & 0 \\ -\frac{3}{4} & -\frac{7}{4} & -\frac{3}{4} & \frac{9}{4} \end{pmatrix}. \quad (34)$$

The remainder  $C_C + C_U$  depends on the lattice action and we give it for three cases: (a) Asqtad fermion and

improved gauge action, (b) Asqtad fermion with plaquette gluon action, (c) standard action, no improvement. The reason for splitting the remainder into two pieces which are not separately gauge invariant, is as follows. Occasionally, simulations are performed with operators that are obtained by dropping the links that connect fermions on different sites. The simulations with these gauge non-invariant operators are performed in Landau gauge and their matching coefficients can be extracted from our calculation. To obtain them, we need to account for the contributions from graphs 1 – 3 in Fig. 1, the wave function renormalization contributions as well as the tadpole improvement for the wave function given in (28). We denote the corresponding matching matrix by  $C_C$ . The remainder, denoted by  $C_U$  is the contribution from graphs 4 and 5 which arises from the link fields in the current operator and the operator tadpole improvement term given in (27). We give the matrices  $C_{C,U}$  in Landau gauge; their sum is gauge invariant.

For the Asqtad and improved gauge action, we find

$$C_C^{(1a)} = \begin{pmatrix} 2.83(14) & -0.75 & 0.38(1) & -1.15(2) \\ -1.25(1) & 4.33(10) & -0.58(1) & -1.34(3) \\ 0.38(1) & -1.15(2) & 2.59(15) & -0.75 \\ -0.58(1) & -1.34(3) & -1.34(2) & 4.36(10) \end{pmatrix}, \quad (35)$$

$$C_U^{(1a)} = \begin{pmatrix} 2.08(5) & 0 & 0 & 0 \\ 0.29 & 0.98(3) & 0 & 0 \\ 0 & 0 & 0 & 0 \\ 0 & 0 & -0.20(1) & 1.14(3) \end{pmatrix}.$$

These results are obtained after tadpole improvement with the “mean link in Landau gauge” definition of the improvement parameter,  $u_0^{(1)} = 0.750(2)$  for the improved gluon action and  $u_0^{(1)} = 0.97432$  for the unimproved action. For Asqtad with the standard plaquette gluon action, the result is

$$C_C^{(1b)} = \begin{pmatrix} 2.33 & -0.75 & 0.34 & -1.03 \\ -1.18 & 3.61(1) & -0.51 & -1.20 \\ 0.34 & -1.03 & 2.09 & -0.75 \\ -0.51 & -1.20 & -1.27 & 3.64(1) \end{pmatrix}, \quad (36)$$

$$C_U^{(1b)} = \begin{pmatrix} 2.97 & 0 & 0 & 0 \\ 0.32 & 1.43 & 0 & 0 \\ 0 & 0 & 0 & 0 \\ 0 & 0 & -0.20 & 1.60 \end{pmatrix}.$$

Notice that case (b) is not equivalent to what is considered in [16]. These authors employ a different discretization of the operators using insertions of fattened links to make the operators gauge invariant while we are using thin links. Also, their fermion action is similar but not identical to the fermion part of the Asqtad action.



Without any improvement terms in the action, we get

$$C_C^{(1c)} = \begin{pmatrix} -0.81 & -0.75 & 0.18 & -0.54 \\ -0.85 & -0.5 & -0.27 & -0.63 \\ 0.18 & -0.54 & 0.25 & -0.75 \\ -0.27 & -0.63 & -0.46 & -0.63 \end{pmatrix}, \quad (37)$$

$$C_U^{(1c)} = \begin{pmatrix} 3.83 & 0 & 0 & 0 \\ 0.47 & 1.86 & 0 & 0 \\ 0 & 0 & 0 & 0 \\ 0 & 0 & -0.38 & 2.14 \end{pmatrix}.$$

The matrices for the unimproved action agree with the known results in the literature [15, 16].

We write the finite correction to the normalization of the axial-vector current in the form  $Z_A = 1 + \frac{\alpha_s}{\pi} \delta Z_A$  and obtain

$$\delta Z_A^{(a)} = 1.17(7), \quad \delta Z_A^{(b)} = 0.921, \quad \delta Z_A^{(c)} = 0. \quad (38)$$

The current renormalization happens to be identical for the gauge invariant and non-invariant operators in Landau gauge. This occurs because in this gauge, the contribution of the fourth graph vanishes and the contribution from fifth graph gets canceled by tadpole improvement.

## VI. SUMMARY AND DISCUSSION

We have calculated the matching of the Wilson coefficients in the  $\Delta S = 2$  flavor changing effective Hamiltonian from the continuum to the lattice for the Asqtad lattice action. Together with non-perturbative calculations of the  $K - \bar{K}$  matrix element of the lattice operators, our results determine the amount of indirect CP violation in the kaon system. The matrix elements are currently being evaluated by the HPQCD and UKQCD collaborations [11, 12]. The calculation uses the configurations with  $n_f = 2 + 1$  dynamical flavors generated by the MILC collaboration.

Previous calculations of the quantity  $B_K$ , which determines the strength of  $K - \bar{K}$  mixing, were performed in the quenched approximation. This induces an essentially unknown and irreducible systematic error into the result. Precise simulations with *dynamical* fermions are necessary in order to be able to make full use of the experimental data on  $K - \bar{K}$  mixing to constrain the CKM matrix elements entering the effective Hamiltonian. Among the currently available fermion actions, only staggered actions allow for simulations with low statistical errors at small quark masses. However, the unimproved staggered action suffers from large taste-changing interactions. The Asqtad action, for which we have performed the matching, has been designed to reduce these as well as other cut-off effects.

We have performed our calculation with two independent methods. First, we have evaluated the diagrams in two different ways: by directly calculating the various diagrams and by first separating off the part which

can be inferred from the renormalization of the current operators. Second, we have evaluated the lattice integrals both algebraically and numerically. For the algebraic evaluation, we have expanded the diagrams around the continuum limit. This produces a set of lattice tadpole integrals which we then reduced to a minimal set of master integrals using computer algebra. The agreement between these two rather different methods provides a strong check on our results.

We find that the size of one-loop corrections to the tree level matching for the Asqtad action is very similar to what is found with unimproved staggered and other improved staggered actions, such as the HYP action [32]. In quenched calculations at a lattice spacing  $1/a = 1.6$  GeV, the shift in the value of the bare  $B_K$  due to  $\mathcal{O}(\alpha_s)$  corrections is around 10% for all these actions [12]. In dynamical simulations with the Asqtad action the shift turns out to be over 15% at the same lattice spacing, simply because the value of the strong coupling is much larger for  $n_f = 3$  than for  $n_f = 0$  dynamical flavors. Also, it turns out that the values for the matching coefficients are not very sensitive to the improvement of the gluon action. Switching off the gluon improvement terms in the Asqtad action changes the entries of the one-loop matching matrix by less than 20% and the changes are even smaller for the larger elements on the diagonal. The motivation for using an improved staggered action in the calculation of  $B_K$  is not to reduce the size of the one-loop corrections, which are already small in the unimproved case, but to correct the large  $\mathcal{O}(a^2)$  scaling violations that highly affect the unimproved case; see [11, 12] for further discussion.

The situation is different for the calculation of other weak matrix elements relevant in the study of CP-violating effects in the kaon system. For the unimproved staggered action, Sharpe and Patel [20] found very large perturbative corrections for operators with scalar and tensor Dirac structure. The contributions are large even after tadpole improvement, which casts doubt on the perturbative expansion for the unimproved action. The corrections are reduced to an acceptable level with the HYP action [33] and operators which are made gauge invariant by the insertion of fattened links [16, 34]. In order to check whether these large corrections are present for the Asqtad action with standard four-quark operators, we have analyzed the mixing of scalar operators. We find that the corrections are small with the improved action. The suppression arises because the improvement terms reduce taste-changing interactions. In Appendix A we present the results for the mixing of scalar operators and discuss the suppression of the large contributions in more detail.

The absence of anomalously large one-loop corrections suggests that the two-loop corrections to our results should be reasonably small. However, in order to reduce the uncertainty in dynamical calculations to the level of a few per-cent, a two-loop matching calculation will be necessary.

**Acknowledgments** We are grateful to Christine Davies and Andreas Kronfeld for discussions and comments on the manuscript. We thank the KITP in Santa Barbara and the INT in Seattle where part of this work was carried out for their hospitality and financial support. This research was supported in part by the U.S. Department of Energy contracts DE-AC02-76CH03000, DE-FG03-94ER-40833 and the Outstanding Junior Investigator Award DE-FG03-94ER-40833, and by the Alfred P. Sloan Foundation. E.G. is indebted to the European Commission for a Marie-Curie Grant No. MEIF-CT-2003-501309. Fermilab is operated by Universities Research Association Inc., under contract with the U.S. Department of Energy.

## APPENDIX A: MIXING OF SCALAR OPERATORS

In this appendix we evaluate the matching for the operators

$$\begin{aligned} Q_1^S &= (\bar{\psi}_1^a \psi_2^a)_S (\bar{\psi}_3^b \psi_4^b)_S, \\ Q_2^S &= (\bar{\psi}_1^a \psi_2^b)_S (\bar{\psi}_3^b \psi_4^a)_S, \end{aligned} \quad (\text{A1})$$

where the bilinears  $(\bar{\psi}_i^a \psi_j^a)_S$  have unit Dirac and taste structure,  $\gamma_S \otimes \xi_T = 1 \otimes 1$  (or equivalently  $\gamma_5 \otimes \gamma_5$ ). These operators are not needed for the evaluation of  $B_K$ , but scalar and pseudoscalar operators are present in the  $\Delta S = 1$  effective Lagrangian used to determine  $\varepsilon'$ . The scalar operators mix into tensor operators under renormalization, but the form of this mixing is not important for our discussion.

For gauge non-invariant operators, the above matching has been studied by Sharpe and Patel [20], who find very large perturbative corrections for these operators even after tadpole improvement. Such large corrections are absent for the HYP action [33] with operators which are made gauge invariant by the insertion of fattened links [16, 34]. As we show below, this is true also for the Asqtad action with standard operators.

Using the same notations and conventions as in Section V, the  $2 \times 2$  matrix for the anomalous dimension of the operators in (A1) is

$$\gamma^{(1)} = \begin{pmatrix} 4 & 0 \\ \frac{3}{2} & -\frac{1}{2} \end{pmatrix}. \quad (\text{A2})$$

After tadpole improvement, the corresponding matching matrices for the unimproved action are

$$C_C^{(1c)} = \begin{pmatrix} -17.26 & 0 \\ -6.28 & 1.59 \end{pmatrix}, \quad (\text{A3})$$

$$C_U^{(1c)} = \begin{pmatrix} 0 & 0 \\ -2.45 & 2.83 \end{pmatrix}.$$

The one-loop correction to the matching is indeed very large, in particular for the element that describes the mixing of  $Q_1^S$  into itself. The large correction is entirely due to the first diagram in Fig. 1. It is twice the renormalization of the scalar current. Note that the operator  $Q_1^S$  is completely local. In terms of the naive field, it is simply

$$\bar{q}(1 \otimes 1) q = \frac{1}{16} \sum_A \bar{\psi}(A) \psi(A). \quad (\text{A4})$$

This implies that for the unimproved action large values are obtained, independently of the prescription adopted to make the operators gauge invariant.

The values obtained for the Asqtad action are

$$C_C^{(1a)} = \begin{pmatrix} -1.8(1) & 0 \\ -0.6(1) & 3.6(1) \end{pmatrix}, \quad (\text{A5})$$

$$C_U^{(1a)} = \begin{pmatrix} 0 & 0 \\ -1.81(1) & 1.68(3) \end{pmatrix}.$$

It is comforting to see that the corrections are smaller with the improved action. The dramatic reduction is mostly due to the fat-link terms in the fermion action.

The origin of the large corrections for the unimproved action, such as those in (A3), has been analyzed by Golterman [35]. He splits the integration region for the loop momenta  $\pi < k_\mu \leq \pi$  into a region around zero  $\pi/2 < k_\mu \leq \pi/2$  and a remainder which contains the corners of the Brillouin zone. For Wilson fermions, he finds that after tadpole improvement the main contribution arises from the integration region around zero. For staggered fermions, on the other hand, large corrections arise from the corners of the Brillouin zone. In this region, the gluon propagator is off-shell, but the staggered fermion propagator has poles.<sup>3</sup> Because the gluon propagator is far off-shell, the first graph in Fig. 2 can be viewed as a fermion tadpole in the corner region. This is the interpretation put forward by Golterman.

The reason for the reduction achieved with the improved action is that the improved quark gluon coupling is designed to suppress taste-changing interactions. The quark-gluon interaction switches off if the in- and outgoing tastes differ. This mechanism suppresses the contribution from the corners of the Brillouin zone to the first diagram in Fig. 1, which corresponds precisely to the situation where the taste of the internal quark line is different from the taste of the external line.

To conclude, we find that the anomalously large perturbative corrections present in some cases for the unimproved staggered action are suppressed in the Asqtad results due to the smaller taste-symmetry breaking of this action. We thus expect that the two-loop corrections to our matching calculation will be reasonably small.

<sup>3</sup> Note that the contribution we are talking about is from the region of hard loop momentum; there are no singularities from propagating doublers. Such contributions only arise at higher

order in the expansion in the lattice spacing.

- 
- [1] C. T. H. Davies *et al.* [HPQCD Collaboration], Phys. Rev. Lett. **92**, 022001 (2004) [hep-lat/0304004].
- [2] J. Charles *et al.* [CKMfitter Group], Eur. Phys. J. C **41**, 1 (2005) [hep-ph/0406184]; M. Bona *et al.* [UTfit Collaboration], hep-ph/0501199.
- [3] S. Eidelman *et al.* [Particle Data Group], Phys. Lett. B **592**, 1 (2004).
- [4] S. Hashimoto, hep-ph/0411126.
- [5] M. Wingate, Nucl. Phys. Proc. Suppl. **140**, 68 (2005) [hep-lat/0410008].
- [6] S. R. Sharpe, hep-lat/9811006.
- [7] C. W. Bernard *et al.*, Phys. Rev. D **64**, 054506 (2001) [hep-lat/0104002].
- [8] S. Naik, Nucl. Phys. B **316**, 238 (1989); G. P. Lepage, Phys. Rev. D **59**, 074502 (1999) [hep-lat/9809157].
- [9] K. Orginos, D. Toussaint and R. L. Sugar [MILC Collaboration], Phys. Rev. D **60**, 054503 (1999) [hep-lat/9903032].
- [10] M. Lüscher and P. Weisz, Phys. Lett. B **158**, 250 (1985).
- [11] E. Gámiz, S. Collins, C. T. H. Davies, J. Shigemitsu and M. Wingate [HPQCD Collaboration], Nucl. Phys. Proc. Suppl. **140**, 353 (2005) [hep-lat/0409049].
- [12] S. Collins, C. T. H. Davies, E. Gámiz, J. Shigemitsu and M. Wingate [HPQCD Collaboration], in preparation.
- [13] T. Becher and K. Melnikov, Phys. Rev. D **66**, 074508 (2002) [hep-ph/0207201].
- [14] T. Becher and K. Melnikov, Phys. Rev. D **68**, 014506 (2003) [hep-lat/0302014].
- [15] N. Ishizuka and Y. Shizawa, Phys. Rev. D **49**, 3519 (1994) [hep-lat/9308008].
- [16] W. j. Lee and S. Sharpe, Phys. Rev. D **68**, 054510 (2003) [hep-lat/0306016].
- [17] A. J. Buras, M. Jamin and P. H. Weisz, Nucl. Phys. B **347**, 491 (1990); S. Herrlich and U. Nierste, Nucl. Phys. B **476**, 27 (1996) [hep-ph/9604330].
- [18] F. Gliozzi, Nucl. Phys. B **204**, 419 (1982).
- [19] H. Kluberg-Stern, A. Morel, O. Napoly and B. Petersson, Nucl. Phys. B **220**, 447 (1983).
- [20] S. R. Sharpe and A. Patel, Nucl. Phys. B **417**, 307 (1994) [hep-lat/9310004].
- [21] M. J. Dugan and B. Grinstein, Phys. Lett. B **256**, 239 (1991).
- [22] A. J. Buras and P. H. Weisz, Nucl. Phys. B **333**, 66 (1990).
- [23] S. Herrlich and U. Nierste, Nucl. Phys. B **455**, 39 (1995) [hep-ph/9412375].
- [24] G. Martinelli, Phys. Lett. B **141**, 395 (1984).
- [25] R. Gupta, T. Bhattacharya and S. R. Sharpe, Phys. Rev. D **55**, 4036 (1997) [hep-lat/9611023].
- [26] I. I. Y. Bigi, M. A. Shifman and N. Uraltsev, Ann. Rev. Nucl. Part. Sci. **47**, 591 (1997) [hep-ph/9703290].
- [27] A. Czarnecki, K. Melnikov and N. Uraltsev, Phys. Rev. Lett. **80**, 3189 (1998) [hep-ph/9708372].
- [28] A. H. Hoang, Z. Ligeti and A. V. Manohar, Phys. Rev. Lett. **82**, 277 (1999) [hep-ph/9809423].
- [29] S. J. Brodsky, G. P. Lepage and P. B. Mackenzie, Phys. Rev. D **28**, 228 (1983).
- [30] G. P. Lepage and P. B. Mackenzie, Phys. Rev. D **48**, 2250 (1993) [hep-lat/9209022].
- [31] S. R. Sharpe, A. Patel, R. Gupta, G. Guralnik and G. W. Kilcup, Nucl. Phys. B **286**, 253 (1987); S. R. Sharpe, hep-ph/9412243; W. J. Lee and M. Klomfass, Phys. Rev. D **51**, 6426 (1995) [hep-lat/9412039].
- [32] W. Lee, T. Battacharya, G. T. Fleming, R. Gupta, G. Kilcup and S. R. Sharpe, Phys. Rev. D **71**, 094501 (2005) [hep-lat/0409047].
- [33] A. Hasenfratz and F. Knechtli, Phys. Rev. D **64**, 034504 (2001) [hep-lat/0103029].
- [34] W. j. Lee and S. R. Sharpe, Phys. Rev. D **66**, 114501 (2002) [hep-lat/0208018].
- [35] M. Golterman, Nucl. Phys. Proc. Suppl. **73**, 906 (1999) [hep-lat/9809125].